Exp Brain Res (2005) 165: 239–249
DOI 10.1007/s00221-005-2294-x

RESEARCH ARTICLE

Mark R. Hinder · Theodore E. Milner

Novel strategies in feedforward adaptation to a position-dependent perturbation

Received: 26 October 2004 / Accepted: 27 January 2005 / Published online: 27 April 2005

Abstract To investigate the control mechanisms used in adapting to position-dependent forces, subjects performed 150 horizontal reaching movements over 25 cm in the presence of a position-dependent parabolic force field (PF). The PF acted only over the first 10 cm of the movement. On every fifth trial, a virtual mechanical guide (double wall) constrained subjects to move along a straight-line path between the start and target positions. Its purpose was to register lateral force to track formation of an internal model of the force field, and to look for evidence of possible alternative adaptive strategies. The force field produced a force to the right, which initially caused subjects to deviate in that direction. They reacted by producing deviations to the left, "into" the force field, as early as the second trial. Further adaptation resulted in rapid exponential reduction of kinematic error in the latter portion of the movement, where the greatest perturbation to the handpath was initially observed, whereas there was little modification of the handpath in the region where the PF was active. Significant force directed to counteract the PF was measured on the first guided trial, and was modified during the first half of the learning set. The total force impulse in the region of the PF increased throughout the learning trials, but it always remained less than that produced by the PF. The force profile did not resemble a mirror image of the PF in that it tended to be more trapezoidal than parabolic in shape. As in previous studies of force-field adaptation, we found that changes in muscle activation involved a general increase in the activity of all muscles, which increased arm stiffness, and selectively-greater increases in the activation of muscles which counteracted the PF. With training, activation was exponentially reduced, albeit more slowly than kinematic error. Progressive changes in kinematics and EMG occurred predominantly in the region of the workspace beyond the force field. We suggest that constraints on muscle mechanics limit the ability of the central nervous system to employ an inverse dynamics model to nullify impulse-like forces by generating mirror-image forces. Consequently, subjects adopted a strategy of slightly overcompensating for the first half of the force field, then allowing the force field to push them in the opposite direction. Muscle activity patterns in the region beyond the boundary of the force field were subsequently adjusted because of the relatively-slow response of the second-order mechanics of muscle impedance to the force impulse.

Keywords Motor learning · Internal dynamics model · Arm · Movement

M. R. Hinder · T. E. Milner (✉)
School of Kinesiology, Simon Fraser University,
Burnaby, B.C. V5A 1S6, Canada
E-mail: tmilner@sfu.ca
Tel.: +1-604-2913499
Fax: +1-604-2913040

M. R. Hinder
Perception and Motor Systems Laboratory,
School of Human Movement Studies,
University of Queensland, 4072, Australia

Introduction

A number of recent studies have proposed that feedforward compensation for novel dynamic environments occurs through the gradual formation of an internal model of the task dynamics (Shadmehr and Mussi-Ivaldi 1994; Lackner and Dizio 1994; Flanagan and Wing 1997; Thoroughman and Shadmehr 2000; Scheidt et al. 2000, 2001). Statistical analysis and modeling studies suggest that kinematic error from previous trials drives improvement in feedforward control (Thoroughman and Shadmehr 2000; Scheidt et al. 2001; Donchin et al. 2003). This is consistent with the concept of feedback error learning proposed by Kawato (1990). However, in early exposures to a new environment, when the internal model is inaccurate, impedance control can be used to limit the perturbing effects of the external force (Franklin et al. 2003a; Osu et al. 2002, 2003). It may also

be used when the dynamics are unstable (Burdet et al. 2001) or unpredictable (Takahashi et al. 2001). Adaptation to novel dynamics by means of changes in limb impedance is not predicted by current schemes of internal model formation. Most previous studies have used velocity-dependent force fields, which were active over the entirety of the movement. This makes it almost impossible to detect whether adaptation is entirely due to changes in feedforward commands to compensate for the force field in an anticipatory manner, or includes online feedback to correct for the effects of perturbations in a reactive manner. Furthermore, these studies did not attempt to quantify the relative contribution to adaptation of changes in limb impedance versus changes in the applied force.

In the present study, we aimed to address these issues by employing a position-dependent force field, which was only active for the first 10 cm of a 25-cm movement. The force field generated only lateral forces which varied with the position in the target direction. By activating the force only over the initial portion of the trial, we attempted to determine whether compensation could be achieved by anticipatory feedforward control alone. We used a virtual mechanical guide, interspersed at regular intervals within force field trials, to assess the extent to which subjects attempted to cancel the force field by generating an equal and opposite force. Scheidt et al. (2000) first used such a mechanical guide to study the role of kinematic and dynamic error feedback following adaptation to force fields. Records of muscle activity were used as an indirect measure of muscle impedance. Our results indicate that subjects used a strategy that approximated the force impulse delivered by the force field, but left a substantial kinematic error in the latter portion of the movement. This error was gradually reduced with training through adaptive changes in muscle activation that occurred principally in the portion of the movement where the force field was inactive. There were also clear indications that muscle impedance was initially increased, again primarily in the latter portion of the movement, and that this was gradually reduced but not eliminated with training.

Methods

Nine subjects (five male, four female) participated in this study. All subjects gave informed consent to the procedures, which were approved by the institutional Ethics Review Committee.

Two-dimensional horizontal movement of the elbow and shoulder was studied using the Parallel-Link Direct-Drive Air and Magnet Floating Manipulandum (PFM). Details of its design and operation have been described previously (Gomi and Kawato 1996, 1997). Subjects sat in a chair with a harness to constrain the trunk so that the elbow and shoulder joints could only move in the horizontal plane. The forearm and wrist were held in a thermoplastic splint rigidly attached to the manipulandum, constraining movement to two degrees of freedom. Forces were applied to the hand by means of two torque motors driving the parallel linkage (Fig. 1).

The chair's height was adjusted such that the arm was in approximately 80° abduction. A circular cursor 0.5 cm in diameter, representing the current hand position, was initially positioned in a 2.5-cm start circle, the center of which was located 31 cm directly in front of the shoulder. The cursor, as well as the start and target circles, were projected onto an opaque horizontal screen suspended above the arm, such that subjects could not see their arm during trials.

Subjects made 25-cm horizontal point-to-point movements away from the body along the y-axis (sagittal plane) to a 2.5-cm diameter target circle. The prescribed movement time of 600 ms was indicated by acoustic signals. No force acted on the hand until after movement had been initiated, nor was any force applied by the PFM as subjects moved back to the start position prior to commencement of the subsequent trial. Subjects initiated each trial on hearing the third beep of a series, and tried to complete the movement on the first beep of the second set of three beeps. The last two beeps of the second series indicated the time that the subject should remain in the target circle before returning towards the start position. The final hand position (OK or OUT) and movement duration (OK, LONG, or SHORT) were presented to subjects on a screen. The final position was deemed OK if the cursor ended in the target circle. The duration was deemed OK if it was within ± 100 ms of the desired movement time. Subjects were instructed that their goal was to produce movements that always met the OK criteria. The knowledge of results was presented primarily as incentive for subjects to improve performance. However, all trials, irrespective of whether

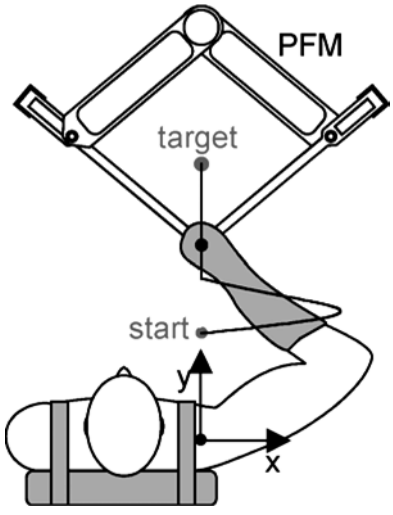

Fig. 1 Plan view of the PFM. Subjects made reaching movements of 25 cm from the start position, located 31 cm from the shoulder. The parabolic force profile is shown schematically. The force acted over the first 10 cm of the movement, with a peak x force of 8 N occurring 5 cm from the start position

the duration and hand position were deemed OK, were used in subsequent data analysis.

A bipolar arrangement of silver–silver chloride disposable electrodes was used for recording surface electromyography (EMG). The surface of the skin was prepared using alcohol wipes, skin abrasion and electrolyte gel to ensure an inter-electrode resistance of less than 10 kΩ. The EMG signals were filtered using a 25 Hz (high pass) and 1 kHz (low pass) filter before sampling at 2,000 Hz. EMG signals were acquired from two monoarticular elbow muscles (brachioradialis and triceps lateralis), two monoarticular shoulder muscles (pectoralis major and posterior deltoid) and two biarticular muscles (biceps brachii and triceps longus). EMG, together with force and position signals, sampled at 500 Hz, were acquired from 400 ms prior to movement onset for 1,400 ms.

The PFM generated a position-dependent force field (PF), as described by the equation:

$$\begin{array}{ll} F_x = -G(y_{\text{start}} - y)(y - y_{\text{end}}), & -(y_{\text{start}} - y)(y - y_{\text{end}}) \geqslant 0 \\ F_x = 0, & -(y_{\text{start}} - y)(y - y_{\text{end}}) < 0 \end{array}$$

where F_x is the force in the x direction (positive to the right), y_{start} and y_{end} define the boundaries of the force field (0 m and 0.1 m), and y is the current location of the hand. G was set at 3,200, to produce a maximum lateral force of 8 N in the PF, which was sufficient to produce a significant lateral perturbation of the hand path.

Training in the PF consisted of 150 trials in which subjects were instructed to stop in the target circle within the specified time window. Every fifth PF trial was replaced by a virtual mechanical guide, which consisted of stiff elastic walls (4,000 N/m) generated by the PFM in the lateral (x) direction on either side of the straight path between the start and target positions, that guided the movements. These trials will be referred to as mechanically-guided trials (GTs). Subjects were not informed about the GTs. Visual feedback was available on each trial, i.e., the cursor representing hand position was visible throughout the task, as were the start and target circles. Since 30 trials in the learning period were GTs, which did not contribute to learning of the PF, only the 120 PF trials were considered in analyzing changes in kinematic error, joint torque and muscle activation associated with learning. We also analyzed the effect of GTs on performance for PF trials which immediately followed, relative to performance on PF trials which immediately preceded them. GTs were used to measure the lateral force that subjects actively produced to counteract the PF.

To analyze trends in EMG as subjects adapted to the PF, we calculated root mean square (rms) EMG over selected time intervals for all PF trials. 'Early rms EMG' was defined as rms EMG in a 300 ms interval beginning 150 ms prior to movement onset. EMG in this early interval represents the feedforward motor command, as well as any stretch reflex activity due to perturbations caused by the PF. Any voluntary amendments to the feedforward command would not be included in this measure. 'Late rms EMG' was defined as rms EMG in the interval beginning 150 ms following movement onset until data collection ceased, 1,000 ms following movement onset. This late interval covered both the latter stages of the movement, including all online responses to the field as well as subsequent stabilization at the target. Baseline rms EMG, computed while the subject was relaxed at the start position, was subtracted from early and late rms EMG prior to further analysis.

To determine the extent to which the rate of adaptation to the PF varied in terms of kinematic error reduction, changes in joint torques, and changes in rms EMG, we fitted exponential decay curves of the form:

$$y = y_{\text{end}} + ae^{-bx}$$

where y represents the value of the variable on any specific trial and y_{end} represents the final adapted error (asymptotic limit of the learning), a and b are constants and x represents trial number. An additional constraint was used such that the fitted curve passed through the data point from the first PF trial, i.e.,

$$y_{\text{end}} + a = y(0).$$

To facilitate this, trials were numbered beginning with PF trial 0. All data were averaged across subjects and normalized to the value on PF trial 0. The 30 GTs were excluded from the exponential fitting procedures, because kinematic error was artificially reduced in these trials, due to the nature of the mechanical guide. Furthermore, it is unlikely that there was any reflex EMG or voluntary EMG associated with error correction during GTs.

Maximum lateral deviation of handpaths from a straight line joining the start and target locations was used to analyze kinematic performance. We restricted this analysis to the region of the trial beyond the PF, i.e., from a distance of 10 cm to 23 cm from the start along the y-axis. In this manner, we restricted the analysis to the portion of each trial where most of the adaptive straightening was seen, while disregarding movement near the target position that included corrective, secondary movements.

To determine the rate of learning in terms of changes in the joint torques, we calculated absolute torque error (Franklin et al. 2003a) for each trial. This measure represents the absolute difference—i.e., area—between the torque profile for a given trial and the final torque profile, calculated as the mean of the final four movements. We used absolute joint torque error, rather than the force recorded against the mechanical guide, to represent adaptation to the PF dynamics. This choice was made because with GTs we only could determine the subject's end *effector* force in isolation from the PF every fifth trial, which may have artificially affected the time constant. By calculating joint torques in the PF, data were available from more consecutive trials.

In the case of the EMG, we fitted an exponential to the early and late rms EMG. We excluded the first three PF trials for all muscles, where EMG was increasing,

since our objective was to determine the time constant of the gradual decrease in rms EMG during training. GTs were also removed, leaving 117 trials for the exponential fit. The rms EMG was still normalized with respect to the first PF trial, to document the amount by which rms EMG increased over the first three trials. The rate at which each variable (handpath error, absolute torque error and rms EMG) was reduced was compared using the time constant τ, calculated as the reciprocal of b in the exponential-fit equation.

Results

Kinematics

Figure 2 shows the handpath kinematics as subjects adapted to the PF. Large rightward lateral deviations on the first trial, which were largest at around 15 cm from the start position, were compensated by *voluntary* corrections in the latter stages of the first trial, such that the target was attained. Subjects quickly learned to compensate for the PF on subsequent trials in a feedforward manner by initiating movements "into" the force field, i.e., subjects' handpaths deviated laterally in the direction opposite to the imposed force, as early as the second or third trial. This leftward deviation persisted throughout the learning period, and was present in the final adaptation. Rightward, lateral deviations in the latter part of the trial, i.e., following removal of the PF, were substantially reduced in the first few trials, and continued to fall for the first 40–50 trials, after which there was little further improvement.

When the PF was replaced by a virtual mechanical guide, hand paths became noticeably straighter, as expected. On PF trials which immediately followed GTs (post-GT trials), we noted an increase in kinematic error, compared to the preceding PF trial (Student's t-test $P < 0.01$) However, performance recovered within one trial, such that maximum lateral deviation in post-GT + 1 trials was not significantly different from that on pre-GT trials ($P > 0.44$) (Fig. 3)

Force recorded in the GTs

Guided trials allowed us to measure lateral forces that were solely due to subjects' active force production without the confounding effect of limb impedance that contributed to force measured on PF trials. Force profiles from the first and last GTs, averaged across all subjects, are shown in Fig. 4. There was substantial modification of the force profile between the first and final GT. Although subjects increased lateral force at a similar rate at the onset of the trial, the maximum force achieved was almost twice as high on the last GT compared to the first GT. Force profiles in the GTs following adaptation did not mirror the PF force profile. At movement onset, subjects produced a force to the left to counteract the force of the PF. Subjects increased their force much more quickly than the PF force increased, such that their force was larger than the PF force for the first 2 cm of the movement. Following the phase of rapidly-increasing force, some subjects reduced their force slightly and then maintained a relatively constant force, whereas others continued to increase their force, but more slowly. The peak subject force was generally 4–5 N, i.e., 3–4 N less than the peak PF force. Subject force dropped more slowly than PF force, such that it was once again larger than the PF force around

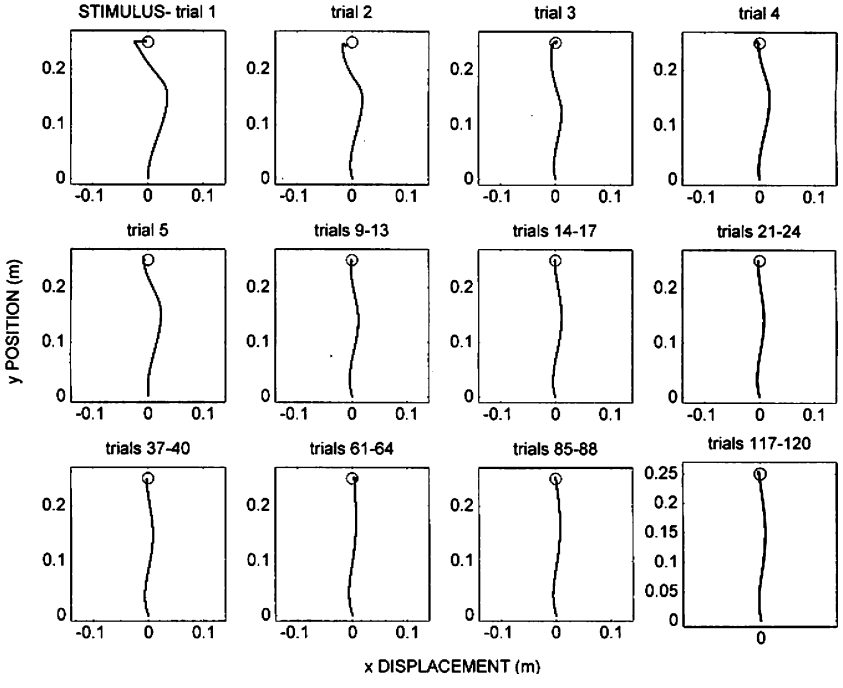

Fig. 2 Kinematic adaptation to the PF. Handpaths in the first five PF trials are shown, along with averages of selected sets of four consecutive PF trials throughout the learning period. The trial numbers refer to the sequence of PF trials, i.e., GTs were not considered as part of the learning period. Hand paths are shown for one subject, but are representative of all subjects

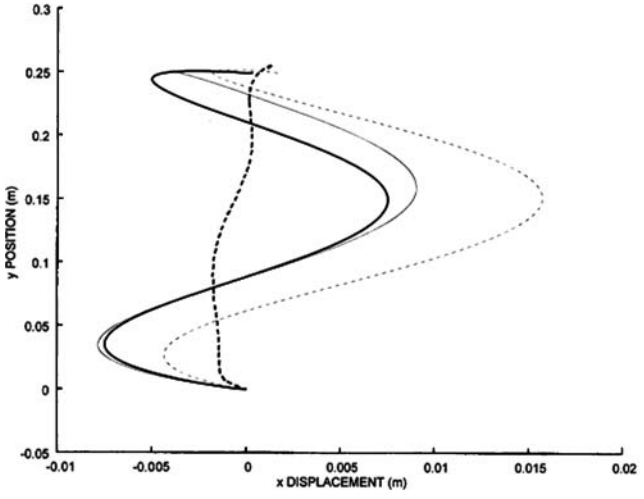

Fig. 3 Degradation of kinematic performance following GT trials. In PF trials prior to GTs (*thin solid line*), subjects moved to the left before being displaced to the right later in the movement. The GT (*thick dotted line*) restricted subjects to a straighter trajectory. On PF trials immediately after GTs (*thin dotted line*), trajectories were displaced farther to the right. However, performance on the next PF trial (*thick solid line*) was similar to the pre-GT trial. Hand paths are shown for one subject, averaged over all trials of a given condition. Note that *x*-displacements are scaled roughly ten times *y*-displacements to exaggerate differences in lateral deviations

8 cm from the start. When the PF boundary was crossed (10 cm from the start) subjects were still exerting a force of 3–4 N to the left. Force crossed zero about 16 cm from the start and subsequently reached a peak value of about 1.5 N to the right (around 19 cm from the start) before returning to zero at the end of the movement.

Figure 5 shows the handpaths in the first and last PF trials, together with the force recorded in the first and last GTs, plotted against time. Although the overall shape of the temporal force profiles does not change, the maximum force that subjects actively produced to compensate for the PF increased with learning, resulting

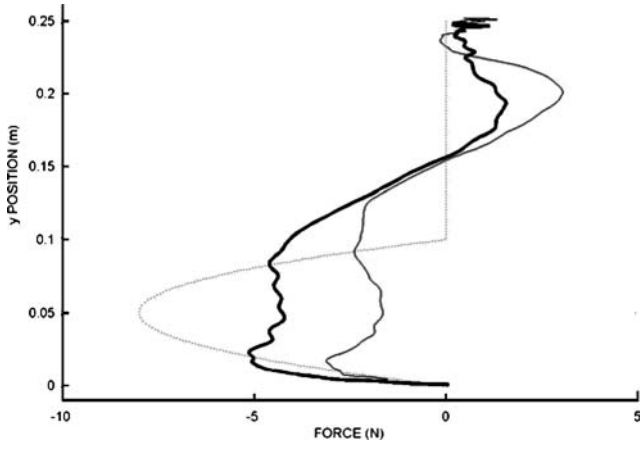

Fig. 4 Force profiles in the initial and final GTs. Force profiles, averaged over all subjects, produced against the GT in the first (*thin line*) and thirtieth (*thick line*) GTs. The PF force profile with its force direction reversed is shown by the *dotted line*

in significantly-lower lateral deviations in PF trials at the end of learning.

To further analyze the subjects' force adaptation, we calculated the force impulse from the force applied to the mechanical guide from 150 ms prior to movement onset until movement reached the PF boundary at 10 cm. Figure 6 shows the evolution of force impulses, normalized to the force impulse of the first GT and averaged across all subjects, for the 30 GTs. We compared force impulses in the first and final GT's of the learning period using a Student's paired *t*-test. We note that as the first GT followed the fourth PF trial, some adaptation to the PF had already occurred prior to the first GT, reducing the ability to capture the full change in adaptation. The *t*-test revealed a significant increase in the force impulse ($P < 0.05$). We found that over all nine subjects the force impulse increased by an average of 59%, with individual subjects increasing force impulse by 8–227%. Linear regression over the 30 GTs was used to determine if there was a systematic change in the force impulse, averaged over the nine subjects. The gradient of the best-fit line was significantly greater than zero ($P < 0.005$), with an R^2 value of 0.26 (Fig. 6), suggesting a systematic increase in the lateral force, although there was considerable variability. The predominant change in force impulse occurred during the first half of the learning period. To demonstrate this, we performed two separate regressions, one for GTs 1–15 and a second for GTs 16–30, and found the gradient of the best-fit line for trials 1–15 was greater than zero ($P < 0.02$) with an R^2 value of 0.33, while the gradient for trials 16–30 was not significantly different from zero ($P > 0.45$).

The profile of the force recorded on GT's corresponded well to the kinematics after adaptation over the first half of the active region of the PF. The lateral deviation to the left reached its peak at about 5 cm, where the subjects' force impulse was approximately equal to that of the PF. The net effect of an equal force impulse is to produce no net change in lateral velocity, i.e., in this case lateral velocity should be zero. Thereafter, the PF force impulse was greater than that of the subjects, corresponding to a reversal in the direction of the velocity and pushing the hand back to the right. The PF force dropped below that of the subjects at about 8 cm, as noted above, and their force impulse ended up approximately equal to that of the PF again at the PF boundary. This should have corresponded to near-zero lateral velocity. In contrast, the lateral velocity on PF trials was close to its peak value in the rightward direction at the PF boundary. This indicates that on GTs subjects exerted a leftward force for much longer than on PF trials. Consequently, we can only assume that GTs accurately represent feedforward commands to muscles until shortly after the PF reaches its maximum force, i.e., about 200 ms after movement onset. As noted above, on GTs subjects' leftward force did not drop to zero until they were about 6 cm beyond the PF boundary. If they had exerted a similar lateral force on PF trials the arm and the PFM would have been driven to

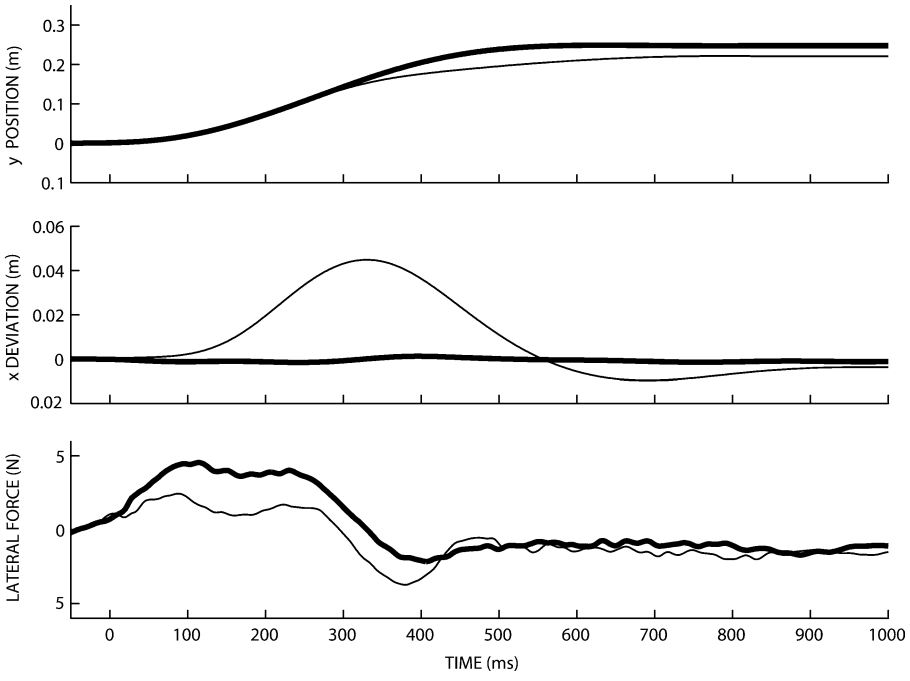

Fig. 5 PF Handpaths and GT force profiles. Hand positions and lateral forces recorded in GTs as a function of time. *x* (*upper panel*) and *y* (*centre panel*) hand positions are shown as a function of time, for the first (*thin line*) and last (*thick line*) PF trials. Temporal lateral-force profiles (*lower panel*) are shown for the first (*thin line*) and final (*thick line*) GTs. Data are averaged across all subjects, and are shown from 50 ms prior to movement onset until data collection ceased, 1,000 ms after movement onset

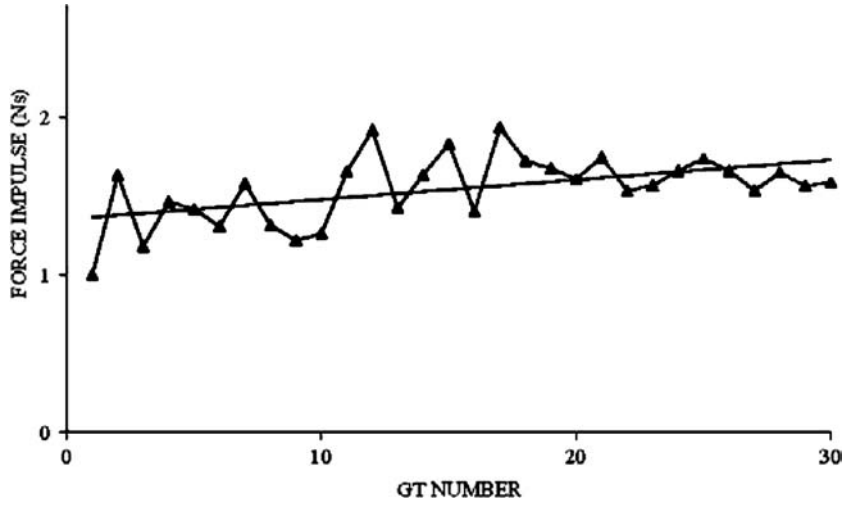

Fig. 6 Force impulse in GTs during PF learning. Force impulses are calculated from 150 ms prior to movement onset until 10 cm (PF boundary). Data is normalized to the first GT and averaged across all subjects. The linear regression revealed a systematic increase in force impulse as subjects adapted to the PF

the left again. However, this was never observed. The rightward force, which was observed even later on GTs, was actually opposite to the leftward movement that subjects produced at the same position on PF trials.

Electromyography

Early rms EMG rose substantially in all muscles in the three trials following the initial exposure to the PF. The increases were most pronounced in the biceps brachii and triceps longus, where activity increased to 2.4 and 2.1 times the corresponding activity in the first PF trial, compared to 1.2–1.7 fold increases in the other muscles. Following the rapid increases, activity generally fell in an exponential fashion over the remainder of the training session. Late rms EMG followed a similar pattern to that of the early rms EMG where generally activity rose over approximately three trials, but to a lesser extent than early rms EMG. An exception to this trend was the pectoralis major, where the highest activity occurred on the first trial. An exponential decrease in the late rms EMG occurred following the initial increase, with the majority of the decrease occurring in the first 50 trials.

Figure 7 shows the averaged EMG of all six muscles for the first and last PF trials. On the first trial, the PF perturbed the arm in such a way as to stretch shoulder and elbow flexor muscles. This induced a stretch reflex response that was initiated slightly before the start of the late EMG interval and was particularly prominent in biceps brachii which is both a shoulder and elbow flexor. At about the same time there was an inhibition of the elbow extensors. Some of the shoulder and elbow flexor EMG in the late interval was probably voluntary

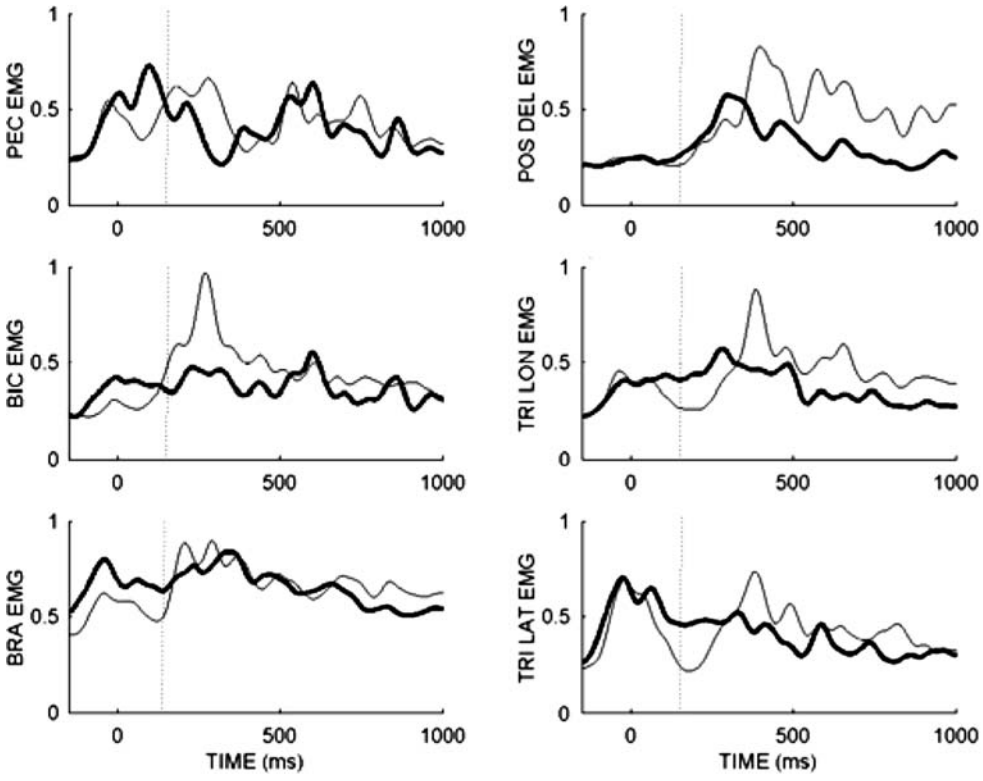

Fig. 7 Muscular activity in the initial and final trials of PF adaptation. EMG is shown for the first (*thin line*) and last—i.e., PF trial 120 (*thick line*)—for all six muscles. Data was normalized to the activity in the first PF trial, and then averaged across the nine subjects. EMG is shown for two shoulder muscles (pectoralis major, PEC, and posterior deltoid, POS DEL; *top panels*), two biarticular muscles (biceps brachii, BIC, and long head of the triceps, TRI LON; *middle panels*) and two elbow muscles (brachioradialis, BRA, and lateral head of the triceps, TRI LAT; *lower panels*). *Vertical dotted lines* show the boundary of the early and late EMG periods, 150 ms after movement onset

correction for the error produced by the PF. However, because the subjects had not yet adapted to the PFM dynamics they overcompensated and ended up to the left of the target (Fig. 2). The very late increase in shoulder and elbow extensor EMG was probably responsible for correction for this overcompensation. Following adaptation, subjects produced greater activation of elbow and shoulder flexor muscles in the early, feedforward portion of the movement than on the first trial, effectively counteracting the force produced by the PF. Because this greatly reduced the perturbing effect of the PF (Fig. 2), pectoralis and biceps brachii EMG in the interval from 150 ms to 400 ms after movement onset were lower after adaptation than on the first trial. Whereas pectoralis EMG appeared to drop to its pre-movement level before increasing later in the movement, biceps brachii EMG remained relatively constant throughout the entire movement. There was little change in the brachioradialis EMG during this interval, and the inhibition of triceps lateralis seen on the first trial disappeared, suggesting stiffening of the elbow by cocontraction. This is also indicated by the similar EMG profiles of triceps longus and biceps brachii, which both remained relatively constant throughout the entire movement following adaptation.

Adaptation time constants

The time constant for the maximum deviation was 2.10 trials, with an R^2 value of 0.90 (Fig. 8a). Thus, on average, it took subjects just two trials to reduce the lateral deviation to 37% of the initial value. Absolute joint torque errors were reduced more slowly than kinematic error. Time constants for the shoulder and elbow absolute joint torque error were 8.77 and 13.01 trials respectively, with R^2 values of 0.63 and 0.85 (Fig. 8b).

Exponential fits for the reduction in early and late rms EMG for all six muscles are shown in Fig. 9. Note that the first data point corresponds to the fourth PF trial. Prior to this the EMG was increasing. This is reflected by the initial value, which is normalized with respect to the rms EMG of the first trial. Time constants for the decline in early rms EMG averaged 13.1 trials, with an average R^2 value of 0.40 (Table 1). In contrast to the relatively rapid decline in early rms EMG, time constants for the late rms EMG were generally longer (average 27.9 trials). In all but one muscle (biceps brachii) the late rms EMG time constant was longer than the early rms EMG time constant (Table 1). R^2 values for the late rms EMG were consistently higher than for the early rms EMG for the corresponding muscle, and averaged 0.71.

Discussion

This study considered the ability of subjects to adapt to a position-dependent force field (PF), which was active over the first 10 cm of a 25 cm reach. We considered adaptation in terms of ability to produce straight

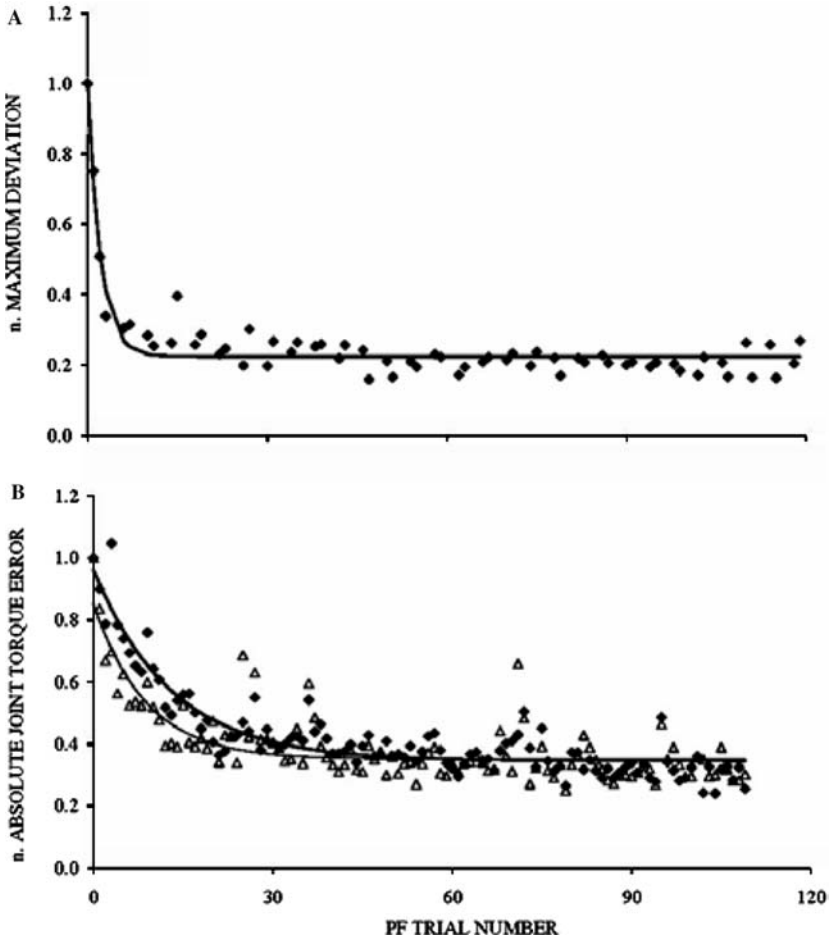

Fig. 8 Exponential decay curves for **a** signed maximum deviation and **b** absolute joint torque errors. Data are averaged over the nine subjects and normalized to the data values of the initial PF trial. The time constant for the signed maximum deviation was shorter than that of the absolute shoulder joint torque error (*open triangles* and *thin line*) and elbow joint torque error (*closed diamonds* and *thick line*)

handpaths, as well as the changes in associated joint torques and EMG activity. Although subjects were able to compensate for the PF, as seen by a rapid reduction in handpath errors, the final adaptation did not result in hand paths quite as straight as those observed in adaptation to other force fields (Burdet et al. 2001; Osu et al. 2003). Even after extensive training, handpaths had an S-shape, bowing to the left in the region of the PF and then bowing to the right over the remainder of the movement. The amount of bowing in the region of the PF following more than 100 trials was similar to that on the second or third trial. In contrast, the amount of bowing in the region beyond the boundary of the PF was greatly reduced in the first few trials and continued to diminish over ~50 trials.

Mechanism of adaptation to the PF

We found that most of the adaptation to the PF, in terms of path straightening and changes in muscle activity, occurred in the region beyond the boundary of the force field. We surmise that this may have been due to the way in which the mechanical impedance of the arm transformed the force impulse of the PF into displacement of the arm. To investigate this idea, we modeled the mechanical response of the arm using appropriate parameter values for inertia, damping and stiffness of the arm taken from Perreault et al. (2004). Modeled as a second-order mechanical system, the impedance of the arm transforms the force of the PF into a smooth lateral displacement of the hand that reaches its peak about 80 ms after the peak force and continues for about 250 ms after crossing the PF boundary. Since peak PF force occurred about 200 ms after movement onset and the PF boundary was reached about 50 ms later, had subjects relied only on the impedance of the arm to counteract the PF they would have experienced a maximum lateral displacement of about 3 cm shortly after crossing the PF boundary, and would not have returned to the original trajectory before reaching the target position, therefore missing the target. By stiffening the arm through cocontraction, the maximum displacement could have been reduced to about 2 cm and the original trajectory regained near the target position. However, it is clear that subjects did more than this, since the maximum displacement was reduced to less than 1 cm.

Force impulses on GT's increased progressively with training, which, together with the reduction in kinematic error, supports the conclusion that subjects formed some type of internal model of the task dynamics, although

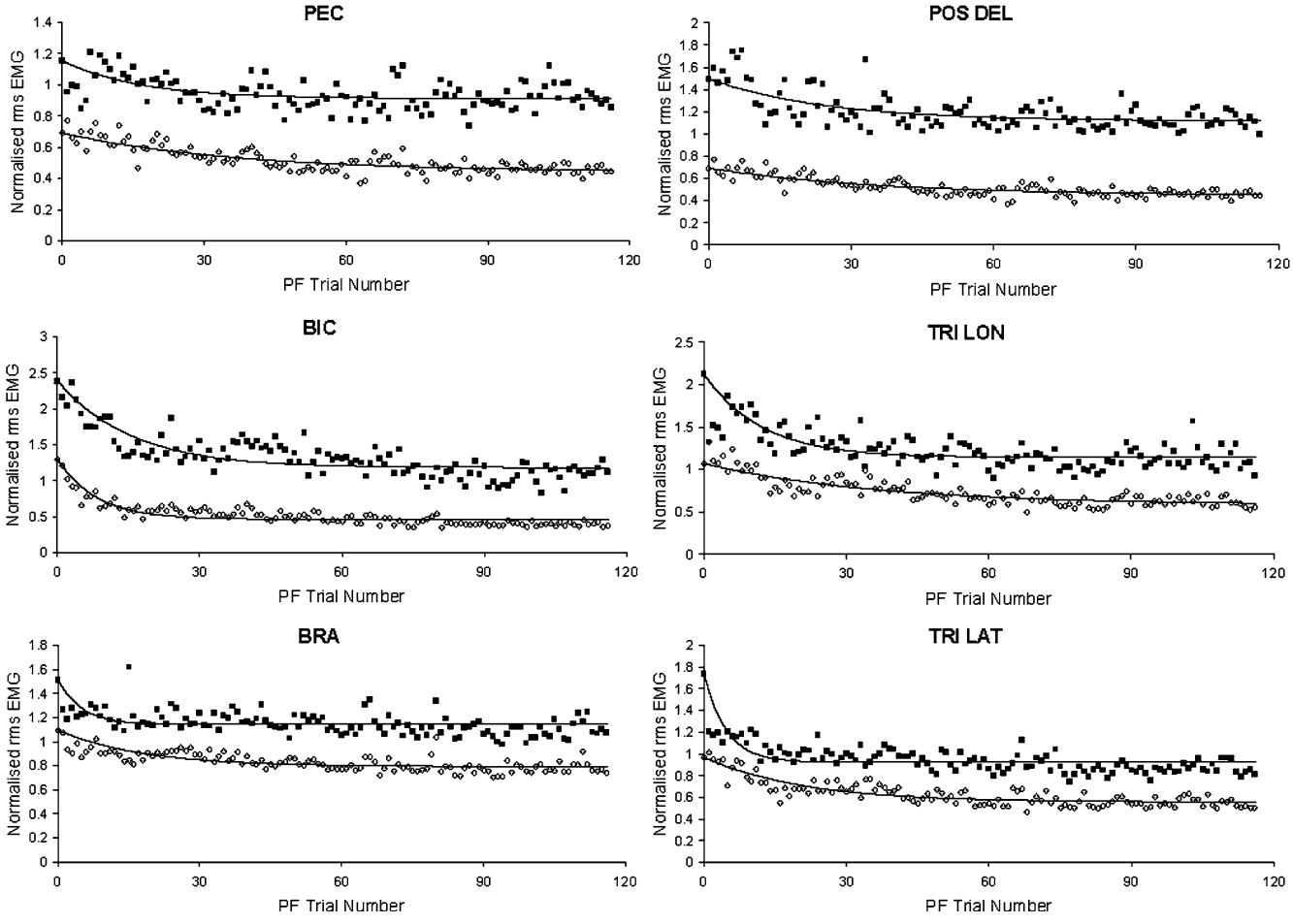

Fig. 9 Exponential decay curves for rms EMG in the early (*squares*) and late (*diamonds*) periods of the PF trials. Initial increases, relative to the first PF trial, were larger in the early period than the late period of the trial, and reached maximum values by the fourth PF trial, shown as the first data point in the fits. Subsequent exponential decreases were generally faster in the early period than in the late period. Data are averaged across the nine subjects, and normalized to the first PF trial (not shown) *PEC* pectoralis major, *POS DEL* posterior deltoid, *BIC* biceps brachii, *TRI LON* triceps longus, *BRA* brachioradialis and *TRI LAT* triceps lateralis

the model did not correspond to the force profile of the PF. EMG in the early portion of the movement, representing the feedforward command, increased in all muscles following the first trial, corresponding to an increase in the impedance of the arm. More specific changes in muscle activation were used to modify torque to generate lateral force to partly cancel the effect of the PF. Following the third trial, the activity in all muscles began to be reduced in an exponential manner. EMG in the later portion of the movement changed similarly with training, although for most muscles it decreased more slowly than in the early portion of the movement. The final level of activity in elbow and biarticular muscles suggested that cocontraction was used to stiffen the elbow over a considerable portion of the movement.

Table 1 Time constants for the exponential fits of rms EMG. Time constants represent averages over the nine subjects

Muscle	τ early rms EMG (trials)	τ late rms EMG (trials)
Pectoralis major	16.6	37.3
Posterior deltoid	24.7	46.5
Biceps brachii	15.6	8.2
Triceps longus	12.1	36.5
Brachioradialis	5.0	18.0
Triceps lateralis	4.6	21.1

Our data is in agreement with numerous previous studies indicating that subjects form internal representations of the task dynamics when adapting to velocity-dependent force fields (Shadmehr and Mussi-Ivaldi 1994; Lackner and Dizio 1994; Flanagan and Wing 1997; Thoroughman and Shadmehr 2000; Scheidt et al. 2000, 2001). A study by Lai et al. (2003) considered adaptation to position-dependent force fields of varying strengths. After-effects were found for all force-field strengths, suggesting that internal models are formed for position-dependent fields, in a similar manner to velocity-dependent fields. Our results indicate that subjects did not form an accurate model of the PF dynamics. Forces exerted during GT's indicate that subjects increased their lateral force as the PF force increased, but at a faster rate. However, their peak lateral force was considerably less than that of the PF, suggesting that

they relied partly on the mechanical impedance of the arm to resist lateral displacement of the hand by the PF. This supposition is supported by evidence of cocontraction of elbow flexor and extensor muscles.

We found that the rate of adaptation to the PF was faster for kinematic error than for torque error and EMG. Maximum deviation from a straight line between target positions was reduced very quickly. Absolute joint torque error, which was used to represent changes in the shoulder and elbow torque, declined more slowly than the kinematic error. Although the rms EMG of some muscles in the early (feedforward) portion of the movement was reduced quite quickly, in general the time constants were similar to those of the torque error. In contrast, except for the biceps brachii muscle, the rms EMG of the late (feedback) portion of the movement decreased more slowly. The time constants for joint torque and changes in EMG are similar to those reported by Franklin et al. (2003a), suggesting that subjects in both studies adapted to the respective force fields in a similar manner.

Adaptation may be limited by neuromuscular constraints

Although subjects were capable of increasing force quickly, they did not match the spatial or temporal profile of the PF. Subjects accelerated their arm in the target direction while simultaneously compensating for the force field. It may have been difficult to coordinate muscle activation such that movement occurred at the desired speed and in the desired direction while simultaneously compensating for the force field. This may be one of the reasons why cocontraction was used in conjunction with the formation of an internal model. Path straightness may have been constrained by limitations in the ability to activate or deactivate individual muscles at different rates, effectively imposing limitations on the ability to compensate for the PF.

Movement trajectories from previous experiments, where subjects performed the same movement while adapting to other types of force fields (Burdet et al. 2001; Osu et al 2003) were straighter than the adapted trajectories in the present study. For seven of the nine subjects who also participated in a concurrent study involving movements in a null field we computed the joint torque profiles required to move through the PF along the same average path as observed for movements in a null field. We found that shoulder torque would have to decrease faster than it increased, while elbow torque would have to decrease more slowly than it increased, unlike the torque profiles for either force-field or null-field movements in previous studies. In our case, the computed torque profiles for shoulder and elbow were oppositely skewed. Although muscle-twitch forces are asymmetric, with shorter (faster) rise times than fall times, different temporal torque patterns at single joints can be achieved by varying the timing and relative amplitude of reciprocal activity in antagonistic muscles (e.g., Brown and Cooke 1990). However, there has been no demonstration that oppositely-skewed torque profiles can be simultaneously generated at the shoulder and elbow. Biceps brachii and triceps longus are biarticular muscles, responsible for generating torque at both joints. Given that these muscles probably contribute a significant proportion of the total joint torque at the shoulder and elbow, oppositely-skewed profiles could probably not be achieved unless the control of single-joint muscles was completely independent of the control of biarticular muscles. Interestingly, actual joint torque profiles following adaptation to the PF show some evidence of a compromise solution to this problem. Shoulder torque decreases too slowly and elbow torque too quickly, compared to the values required for a straight movement. Furthermore, the activity of the biarticular muscles changes in parallel, and remains relatively constant throughout most of the movement, perhaps not only to increase joint stiffness but also to avoid counteracting the potential ability of monoarticular muscles to create asymmetric torque profiles. Had we permitted subjects to move more slowly to reduce muscle activation and deactivation rates, differences in the shape of torque profiles produced by single joint and biarticular muscles would have been reduced, and straighter hand paths could probably have been achieved.

Simultaneous use of internal models and cocontraction

The bowing of trajectories in the early part of movements, characterized by lateral movements "into" the field, suggests that subjects were able to anticipate and compensate for the perturbing effects of the PF as early as the second or third trial. Subjects produced an initial lateral force large enough to overcome the PF, enabling the inertial mass of the arm and PFM to be accelerated laterally. This initial overcompensation reduced the trajectory error that would otherwise have occurred in the later portion of the movement, i.e., due to the delayed effect of the PF force, arising from the low-pass filtering of the force impulse by the second-order mechanics of the arm's mechanical impedance.

Activation of all muscles was progressively reduced as subjects adapted to the PF. Since performance did not become worse as the rms EMG dropped, we can assume that they were reducing the mechanical impedance of the arm because they had learned to counteract the PF by appropriately modulating elbow and shoulder torque. We suggest that subjects reduced the stiffness of the arm to an optimal level (Franklin et al. 2004), which represented compensation for trajectory error resulting from the inability to achieve an accurate internal model of the PF through reciprocal activation of monoarticular muscles, perhaps because of mechanical limitations or high metabolic cost. Our results support previous studies which suggest that internal model formation and impedance control are both used during adaptation to

novel dynamics (Takahashi et al. 2001; Franklin et al. 2003a, 2003b; Osu et al. 2002). It appears, as Osu et al. (2002) suggest, that cocontraction is initially high, when the internal model is inaccurate, but is reduced as feedforward commands more accurately compensate for the external dynamics.

Acknowledgements This work was conducted while M.R. Hinder worked as a student intern in the Computational Neuroscience Laboratories at Advanced Telecommunications Research Institute International, Kyoto, Japan. We thank Dr. M. Kawato for this opportunity. We also thank D. Franklin and T. Yoshioka for assistance in conducting experiments at ATR, and D. Franklin for providing an earlier version of Figure 1. This work was supported in part by the Natural Sciences and Engineering Research Council of Canada and the Gordon Diewert Memorial Scholarship.

Appendix

Simulations to determine how the impedance of the arm transformed the force impulse of the PF into lateral displacement were carried out using a second-order model of the limb mechanics driven by joint torques, τ_r, derived from null-field movements such that

$$I(\theta)\ddot{\theta} + C(\theta,\dot{\theta})\dot{\theta} + B_j\dot{\theta} + K_j(\theta - \theta_r) = \tau_r + \tau_{PF}$$

where I represents the inertia of the arm determined from anthropometric estimates, C represents Coriolis and centrifugal terms, B_j is the joint damping matrix, K_j is the joint stiffness matrix, $\theta_r(t)$ is the null field trajectory and τ_{PF} represents the joint torques imposed by the PF. Joint stiffness terms were scaled as a function of joint torque, corresponding to measurements made by Osu and Gomi (1999) and Perreault et al. (2004). Joint damping was proportional to joint stiffness and inversely proportional to joint velocity (Tee et al. 2004), with a proportionality constant chosen such that the damping ratio was approximately equal to that measured by Perreault et al. (2004). Joint torques, τ_r, were computed from inverse dynamics, using the trajectories and the hand forces recorded during null-field movements as in Franklin et al. (2003a). The above differential equation was solved using the Matlab function ode45.

References

Brown SH, Cooke D (1990) Movement-related phasic muscle activation. I. Relations with temporal profile of movement. J Neurophysiol 63:455–465

Burdet E, Osu R, Franklin DW, Milner TE, Kawato M (2001) The central nervous system stabilizes unstable dynamics by learning optimal impedance. Nature 414: 446–449

Donchin O, Francis JT, Shadmehr R (2003) Quantifying generalization from trial-by-trial behaviour of adaptive systems that learn with basis functions: theory and experiments in human motor control. J Neurosci 23:9032–9045

Flanagan JR, Wing AM (1997) The role of internal models in motion planning and control: evidence from grip force adjustments during movements of hand-held loads. J Neurosci 17:1519–1528

Franklin DW, Osu R, Burdet E, Kawato M, Milner TE (2003a) Adaptation to stable and unstable dynamics as achieved by combined impedance control and inverse dynamics model. J Neurophysiol 90:3270–3282

Franklin DW, Burdet E, Osu R, Kawato M, Milner TE (2003b) Functional significance of stiffness in adaptation to stable and unstable dynamics. Exp Brain Res 151:145–157

Franklin DW, So U, Kawato M, Milner TE (2004) Impedance control balances stability with metabolically costly muscle activation. J Neurophysiol 92:3097–3105

Gomi H, Kawato M (1996) Equilibrium-point control hypothesis examined by measured arm stiffness during multijoint movement. Science 272:117–120

Gomi H, Kawato M (1997) Human arm stiffness and equilibrium-point trajectory during multi-joint movement. Biol Cybern 76:163–171

Kawato M (1990) Feedback-error-learning network for supervised motor learning. In: Eckmiller R (eds) Advanced neural computers. North-Holland/Elsevier, Amsterdam, pp 365–372

Lackner JR, Dizio P (1994) Rapid adaptation to coriolis force perturbations of arm trajectory. J Neurophysiol 72:299–313

Lai EJ, Hodgson AJ, Milner TE (2003) Influence of interaction force levels on degree of motor adaptation in a stable dynamic force field. Exp Brain Res 153:76–83

Osu R, Gomi H (1999) Multijoint muscle regulation mechanisms examined by measured human arm stiffness and EMG signals. J Neurophysiol 81:1458–1468

Osu R, Franklin DW, Kato H, Gomi H, Domen K, Yoshioka T, Kawato M (2002) Short- and long-term changes in joint co-contraction associated with motor learning as revealed from surface EMG. J Neurophysiol 88:991–1004

Osu R, Franklin DW, Kato H, Gomi H, Domen K, Yoshioka T, Kawato M (2003) Different mechanisms involved in adaptation to stable and unstable dynamics. J Neurophysiol 90:3255–3269

Perreault EJ, Kirsch RF, Crago PE (2004) Multijoint dynamics and postural stability of the human arm. Exp Brain Res 157:507–517

Scheidt RA, Reinkensmeyer DJ, Conditt MA, Rymer WZ, Mussa-Ivaldi FA (2000) Persistence of motor adaptation during constrained, multi-joint, arm movements. J Neurophysiol 84:853–862

Scheidt RA, Dingwell JB, Mussa-Ivaldi FA (2001) Learning to move amid uncertainty. J Neurophysiol 86:971–985

Shadmehr R, Mussa-Ivaldi FA (1994) Adaptive representation of dynamics during learning of a motor task. J Neurosci 14:3208–3224

Takahashi CD, Scheidt RA, Reinkensmeyer DJ (2001) Impedance control and internal model formation when reaching in a randomly varying dynamical environment. J Neurophysiol 86:1047–1051

Tee KP, Burdet E, Chew CM, Milner TE (2004) A model of force and impedance in human arm movements. Biol Cybern 90:368–375

Thoroughman KA, Shadmehr R (2000) Learning of action through adaptive combination of motor primitives. Nature 407:742–747